ISTITUTO NAZIONALE DI FISICA NUCLEARE

Sezione di Catania

INFN/BE-90/03
25 Gennaio 1990

G. Lanzanò, A. Pagano, E. De Filippo, R. Dayras and R. Legrain:

THE ABLATION STAGE IN THE FAST ABRASION MODEL

Servizio Documentazione
dei Laboratori Nazionali di Frascati

INFN - Istituto Nazionale di Fisica Nucleare
Sezione di Catania

INFN/BE-90/03
25 Gennaio 1990

The ablation stage in the fast abrasion model

G. Lanzanò, A. Pagano and E. De Filippo
Istituto Naz. di Fisica Nucleare and Dipartimento di Fisica
Corso Italia 57, 95129 Catania, ITALY
R.Dayras, R.Legrain
DPhN/BE, CEN Saclay, 91191 Gif/Yvette Cedex, FRANCE

Abstract

In order to study the effect of the ablation stage on the fast abrasion mechanism, detailed evaporative calculations have been performed on the primary projectile and target-like fragments issued from the reactions $^{40}Ar+^{27}Al$ and $^{40}Ca+^{27}Al$. The obtained results are able to account for many of the experimental features observed in the projectile and target-like fragments produced at intermediate energies. However it is pointed out that, in order to get a better agreement between theory and experimental data, the primary projectile and target-like fragments should carry a more substantial excitation energy than predicted by a purely geometric abrasion model.

1. Introduction

Recently, with the advent of new accelerators operating at intermediate energies, the study of the reaction mechanism involved in projectile fragmentation has received a

renewed interest by physicists. In this aim many experiments have been accomplished at GANIL, showing evidence for a like participant - spectator mechanism [1]. The fast abrasion - ablation model, typical of higher relativistic energies, has been successful in explaining many of the observed experimental gross features of the fragmentation process at these intermediate energies as, for example, in the reactions $^{40}Ar + ^{27}Al, ^{nat}Ti$ at 44 Mev/n [2]. In this model, during the interaction, projectile and target suffer a reciprocal fast removal of nucleons (abrasion stage). As a result, primary excited projectile–like (PLF) and target- like (TLF) fragments emerge essentially cold from the reaction zone, and then decay by emission of particles (ablation stage). The formation or not, in the overlap zone, of an equilibrated, higly excited nuclear system (fire-ball), is up to now a debated question. In a foregoing paper [3] we have described a simple geometrical approach to the fast abrasion model, and have compared with success the obtained simple analytical formulas for some physical measurable observables with recent experimental results. However, as it was stressed in the paper, all the obtained results referred to primary excited fragments, the properties of which can be modified by the ablation stage.

In order to see to which extent the ablation stage can influence the properties of the abraded fragments, we have undertaken a series of detailed evaporative calculations, making some reasonable assumptions, as described in the following paragraph. Next the main results will be presented, and finally some conclusions will be drawn.

2. Abrasion–ablation calculations

Fast abrasion calculations are strictly geometric, and are able to determine, for each fragment, its mass and associated production cross section as a function of the impact parameter. However, evaporative calculations need the knowledge of fragment excitation energy, charge and angular momentum. We shall describe below the method and the approximations made in determining these quantities. Consistently with the notations used in the previous paper [3], we shall indicate with A_{PF},Z_{PF} (A_{TF}, Z_{TF}) respectively the mass and charge of the primary projectile (target)- like fragments, and with A'_{PF}, Z'_{PF} (A'_{TF}, Z'_{TF}) respectively the mass and charge of the projectile (target) - like fragments after the ablation stage. PLF and PLF′ shall stand for primary and final projectile - like fragments respectively.

i) Excitation energy.

At intermediate energies, the problem of determining the excitation energy carried away by the primary fragments is still controversial, as different experiments have given contradictory results [4,5,6]. Furthermore, also from a theoretical approach, two extreme reaction mechanisms can be envisaged to account, equally well, for correlations between PLF and TLF observed in recent experiments [7]. In one of them the reaction is thought to be binary, so that projectile and target are still emerging from the reaction as two well defined, equilibrated and highly excited systems, which then decay by particle emission, giving rise to the observed PLF′ and TLF′. In another one the reaction proceeds by a fast abrasion mechanism, in which a PLF and a TLF are created with low excita-

tion energy, while most of the excitation energy is deposited in the overlap zone of the two nuclei. In the following we shall calculate the excitation energy of the primary fragments in this later context. In the framework of a fast abrasion model this excitation energy can be calculated geometrically through the difference of surface between the abraded fragment of mass A_{TF} and a spherical fragment of the same mass [2] (For approximative formulas, see ref. [8,9,3]). In fig. 1, as an example, the excitation energy of the abraded fragment is reported as a function of its mass, A_{PF} or A_{TF}, for the reaction $^{40}Ar + ^{27}Al$. Starting from the projectile mass, its trend is smoothly increasing as the fragment mass decreases. A drawback of this model is the exceedingly low excitation energy foreseen for masses near the projectile, where, on

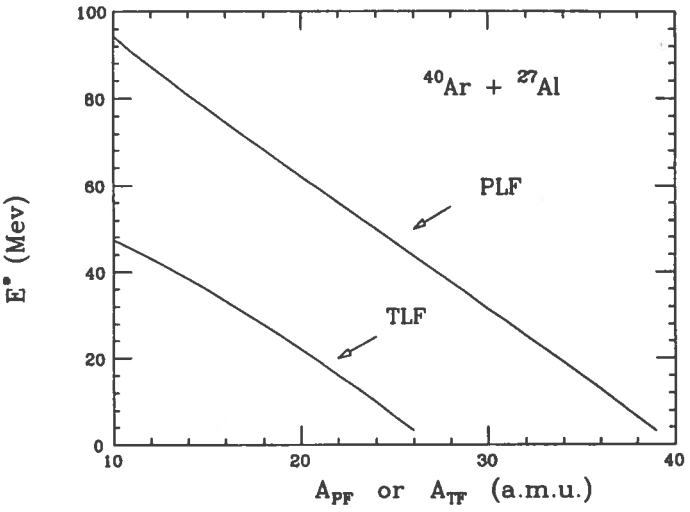

Fig. 1 *Excitation energy of the primary projectile and target-like fragments as a function of their mass*

Tab. I

A_{PF}	$\sigma_A(mb)$	$E^*_{PF}(Mev)$	Z_1	P%	Z_2	P%	Z_3	P%
39	263.6	3.2	17	44.8	18	54.1	19	1.1
38	179.9	6.4	16	5.3	17	79.3	18	15.4
37	142.7	9.5	16	34.5	17	64.0	18	1.5
36	119.5	12.8	15	2.3	16	76.8	17	20.9
35	104.3	15.9	15	23.6	16	74.2	17	2.2
34	92.9	19.1	14	0.7	15	70.9	16	28.4
33	84.1	22.2	14	14.2	15	82.7	16	3.1
32	76.9	25.2	13	0.2	14	62.0	15	37.8
31	70.7	28.4	13	6.9	14	88.5	15	4.6
30	65.6	31.5	13	50.0	14	50.0	--	--
29	61.1	34.5	12	2.5	13	90.6	14	6.9
28	57.1	37.6	12	35.9	13	63.9	14	0.2
27	53.5	40.7	11	0.6	12	88.6	13	10.8
26	50.4	43.7	11	22.1	12	77.7	13	0.2
25	47.4	46.8	10	0.1	11	83.3	12	16.6
24	44.7	49.9	10	10.2	11	89.4	12	0.4
23	42.2	52.9	10	73.6	11	26.4	--	--
22	39.9	56.0	9	3.1	10	96.3	11	0.6
21	37.7	59.1	9	59.1	10	40.9	--	--
20	35.6	62.1	8	0.5	9	98.5	10	1.0
19	33.6	65.2	8	39.7	9	60.3	--	--
18	31.8	68.3	8	98.2	9	1.8	--	--
17	30.0	71.3	7	18.7	8	81.3	--	--
16	28.2	74.4	7	96.2	8	3.8	--	--
15	26.5	77.6	6	4.5	7	95.5	--	--
14	24.8	80.7	6	91.5	7	8.5	--	--
13	23.2	83.9	5	0.2	6	99.8	--	--

the contrary, the exchange of a few nucleons plays certainly a significative role. Recently, Bonasera et al. [10] have used a new approach, in which dissipative effects have been included during the collision,obtaining, in such a way, PLF and TLF much more excited than in the simple geometrical approach.

ii) Charge

Different, model dependent approaches can be used to determine the charge of the primary fragments [11,12,13]. If neutrons and protons are considered not correlated inside the nuclear volume, the so called hypergeometric formula is easily derived, that gives, for each primary fragment of mass A_{PF},the relative charge distribution. On the other hand, coherent motions of neutrons against protons inside the nuclear volume, giving rise to zero point vibrations of GDR, provide also a mean to calculate primary PLF charge distribuition.

The approach that we have chosen is the most appropriate and suited to the fast abrasion model, as described below. Treating, for istance, the case of the PLF, we shall suppose that, on the average, primary PLF has still the same N/Z ratio of the projectile, say $(N/Z)_P$, so neglecting the slight dependence on the target N/Z value, as observed experimentally [14]. The N/Z distribution is then, for each fragment, supposed gaussian, centered around the value $(N/Z)_P$ of the projectile and with a width σ_o, that we treat as a parameter and suppose, for sake of simplicity, not depending on the PLF mass. We can simply estimate σ_o recalling that the charge value is an integer. In fact when a PLF mass matches a unique value of charges in order to reproduce the mean assumed value $(N/Z)_P$, then the indetermination on the charge is $\simeq 0$ and $\sigma_0 = \sigma_0^{min} \simeq 0$ too; on the contrary if two consecutive charge values match equally well the PLF mass in order to reproduce the $(N/Z)_P$ value, then we have an indetermination of ± 0.5 charge unit and σ_0 is maximal. In the latter case, referring to an ^{40}Ar beam and a mean mass value $A_{PF} \simeq 21$ a.m.u., we find a deviation of N/Z from $(N/Z)_P$ that is $\sigma_0^{max} \simeq 0.10$. Averaging between the minimum and the maximum value of σ_0, we obtain $\sigma_0 \simeq 0.05$, that is the value used throughout the calculation. Finally we have calculated, for each PLF mass, the probability of having a certain charge Z_i, using tabulated areas

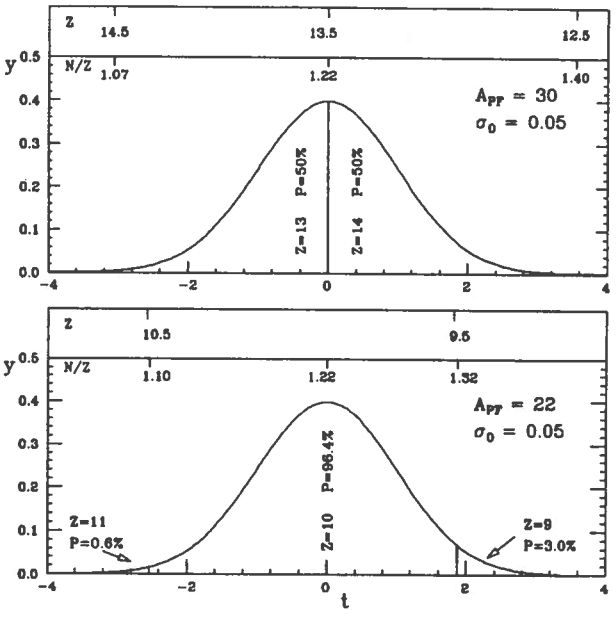

Fig. 2 *Charge probability distribution for A'_{PF} = 30 and 22 a.m.u. respectively*

subtended by a standard gaussian distribution of the form:

$$y = \frac{1}{\sqrt{2\pi}} exp(-t^2/2)$$

where

$$t = \left(\frac{N}{Z} - < \frac{N}{Z} >\right) \Big/ \sigma_0$$

and

$$< \frac{N}{Z} >= \left(\frac{N}{Z}\right)_P \; or \quad \left(\frac{N}{Z}\right)_T$$

depending if the ablation stage was calculated on the PLF or TLF. This is well illustrated in Fig. 2, where these calculated distributions are reported for two typical extreme cases, $A_{PF} = 30$ and $A_{PF} = 22$ respectively. In the former, two charges values (Z=13 and Z=14 respectively) equally share the whole area, normalized to unity, while in the latter case only a charge value (Z=10) is accounting for $\sim 96\%$ of the whole area.

iii) Angular momentum

Studies on the angular momentum carried away by primary PLF are lacking, so that, at moment, no knowledge exists on the PLF angular momentum as a function of its mass. We shall then assume, as currently done, that it is very small, fixing its value to $L = 5\hbar$ throughout the calculations. This assumption will certainly affect the ablation stage since emission of light particles, as protons or neutrons, will be favoured against emission of α particles.

The calculations have been performed using the code CASCADE [15], in which, for each primary PLF, mass, charge, excitation energy and angular momentum were given as inputs. We have studied, in particular, the reaction $^{40}Ar + {}^{27}Al$; the reaction $^{40}Ca + {}^{27}Al$ was also studied in order to see the influence of the projectile charge on the properties of final products. Table I collects, for each PLF, the quantities used in the evaporative calculations, specifically mass, production cross section, excitation energy, charge value with relative probabilities. The production cross section and excitation energy for each mass A_{PF} has been obtained as described above,using the program ABRADE of R. Dayras [16], with a reduced radius parameter r_o=1.36 fm. The primary PLF's charge distribution (relative to a given PLF mass A_{PF}) has been obtained by the above described method and, as it can be seen, only one or two charge values are essentially foreseen for each primary PLF mass. As for the masses greater then $A_{PF} = 37$ a.m.u. the excitation energy was not enough to allow for particle evaporation, while for masses less than $A_{PF} = 13$ a.m.u most of the decay products were essentially very light ions, then we have restricted our calculations from $A_{PF} = 13$ to $A_{PF} = 37$, studying this way the decay products from Z=5 to Z=16. In order to compare the results of the calculation with the experimental ones, we have summed up the production cross sections of a given PLF', resulting as a residual nucleus from the decay of different primary PLFs.

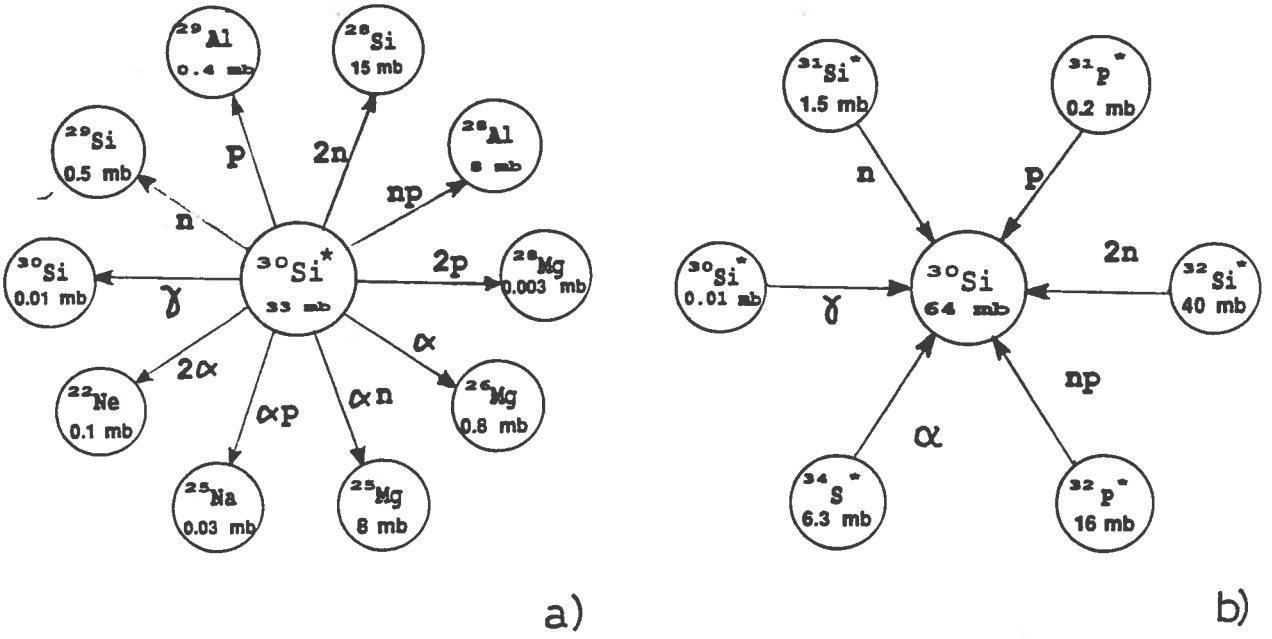

Fig. 3 *Sketch showing a) the decay products for the PLF ^{30}Si excited at 31.5 Mev. b) the primary projectile-like fragments that have, as their final product of decay, a ^{30}Si PLF'. For each decay path the accompanying light charged particles and the relative intensity in mb. are also shown.*

Cross sections of light particles accompanying a given residue have also been taken into account, in order to have an estimation of the light particle multiplicities.

As an example of calculation, fig. 3a gives a sketch of the decay products accompanying the disexcitation of the PLF ^{30}Si excited to 31.5 Mev. Channels involving the emission of one or two neutrons are the most intense. Fig. 3b, on the contrary, gives a sketch of the primary nuclei that contribute to the production of the fragment with $A'_{PF} = 30$ and $Z'_{PF} = 14$, relatively near to the mass of the projectile. As the PLF' mass decreases, the number of primary PLFs feeding it grows and, for instance, as many as 15 different primary PLFs are contributing, with different weight, to the production of a ^{12}C PLF'. This fact will have some consequences on the coincidence experiments, as we shall see in the following.

3. Results

This section will deal with main results extracted from the evaporative calculations, mainly the ones relative to the reactions $^{40}Ar + ^{27}Al$ and $^{40}Ca + ^{27}Al$. When possible, comparison with experimental data obtained at intermediate energies will be made.

a) The $^{40}Ar + ^{27}Al$ reaction

Let us, first, reconsider Fig. 2 and ask us how the ablation stage changes the assumed charge distribution of the primary PLFs. If the ablation stage is not taken into account, the charge distribution of the primary PLFs is also the final one, as indicated by the squares of Fig. 4 a) and b), in which the final charge distribution is reported respectively for the masses A'_{PF}=30 and $A'_{PF} = 22$ a.m.u. The accord of these distributions, in which the N/Z value of the beam is still kept as a mean value, with the experimental one [2]

(black circles) is not good. Taking into account the ablation stage, we obtain the final distribution indicated by open circles, in which the agreement with the experimantal data is always good. A way to summarize these results is reported in Fig. 5, where the ratio $< A'_{PF}/Z'_{PF} >$ is reported as a function of the final fragment mass A'_{PF}. This way of representing the results is more meaningful than the one in which, as customary, the $< N > /Z$ ratio is reported as a function of Z, since on the one hand more enphasis is given to the mass of the final PLF', and on the other hand a more structured pattern can be evidenced. The dashed line rapresents the initial A/Z value of the projectile and hence, on the average, the A/Z ratio for the primary fragments. The theoretical results, indicated by open circles joined by segment lines, are able to reproduce fairly well both the general trend and the large fluctuations seen in the experimental data, especially for masses less than $A'_{PF} = 30$. For higher masses the accord is less good, and this has to be imputed, as said before, to a defect of the model that does not include, for masses near the one of the projectile, a few nucleon exchange mechanism, as experimentally observed [17]. This could increase considerably the excitation energy associated to primary PLF with mass near the one of the projectile. In Fig. 6 the mass distribution for $Z'_{PF} = 14$ and $Z'_{PF} = 8$ respectively is reported as a function of the final mass of the PLF. In general both the shape and the width of the experimental distribution are well reproduced for all the Z'_{PF} ranging from 15 to 5 charge unities. Let us con-

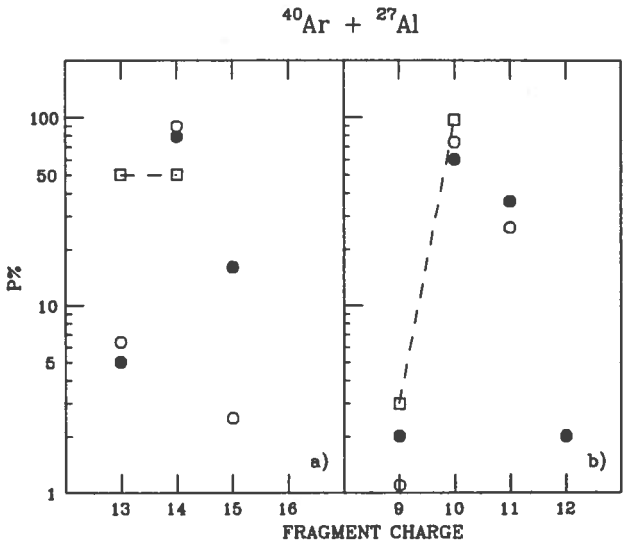

Fig. 4 *Charge distribution relative to the final projectile-like fragments of mass respectively 30 and 22 a.m.u. Experimental points from ref.* [2].

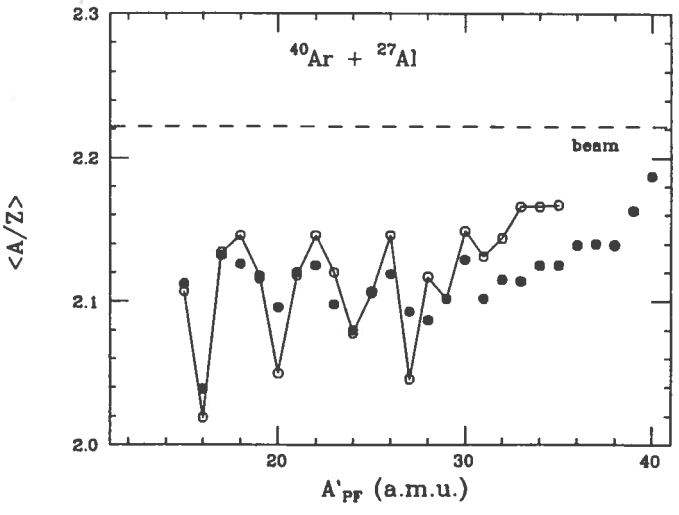

Fig. 5 *The mean ratio between the mass and charge of the final projectile-like fragment is shown as a function of the PLF' mass. The value corresponding to the beam is also shown as a dashed line. Experimental points from ref.* [2].

sider now Fig. 7, in which the PLF′ production cross section is reported as a function of their mass A'_{PF}. The line represents the same cross section after the ablation stage. As compared with the experimental points, the calculation reproduces the general trend, with a minimum around $A'_{PF} = 18$ a.m.u. and a rise of the cross section for masses lower then 18 a.m.u.. Howewer the calculation introduces some important oscillations (fluctuations) that are not observed experimentally. Concerning the bump observed for low values of A'_{PF}, the calculation reproduces it only in part, so that other competing mechanisms are not excluded [18]. With regard to this, notice that calculation predicts maxima in the structure centered at

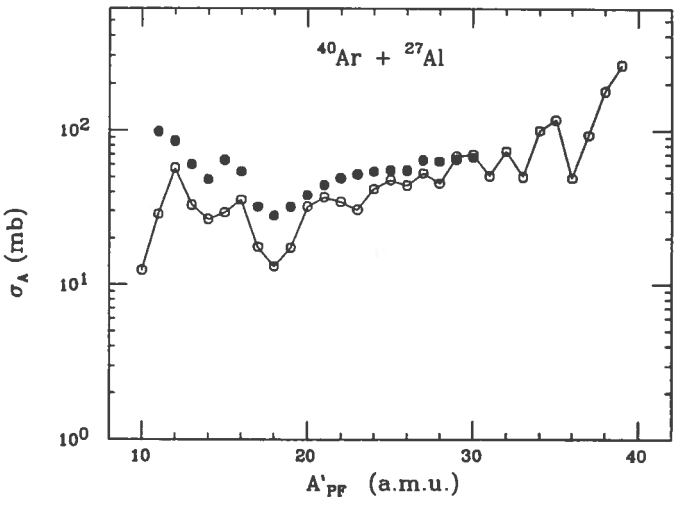

Fig. 7 *Final PLF's production cross section as a function of their mass. Experimental points from ref.* [2].

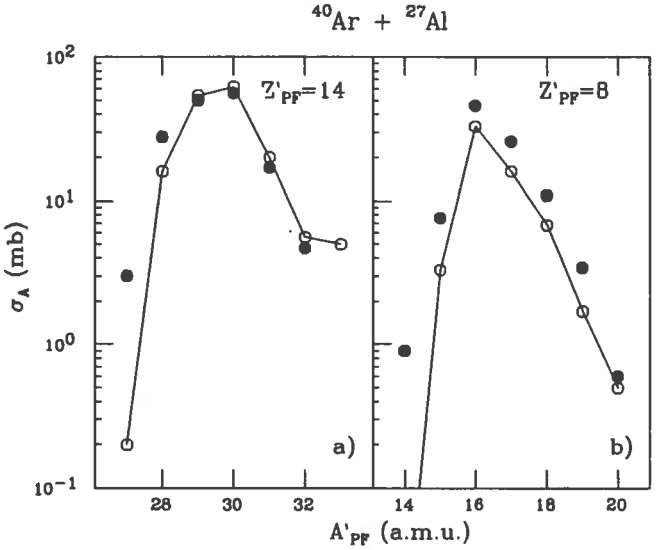

Fig. 6 *Final isotope distribution for projectile-like fragment of charge respectively 14 and 8. Experimental points from ref.* [2].

$A'_{PF} = 12$ and $A'_{PF} = 16$, while experimentally they are centered at $A'_{PF} = 11$ and $A'_{PF} = 15$, indipendently of the target [2,19]. This would suggest a mechanism in which the projectile, in central collision, would fission just before the interaction with the target, giving rise to two excited fragments. Supposing a symmetric fission with low excitation energy (typically ^{20}F at $E^* = 20 - 30$ Mev), the ablation stage subsequent to the creation of the fragments, would enhance mass distributions centered on the isotopes ^{15}N and ^{11}B. Fig. 8 shows the charge production σ_Z as a function of the observed charge Z'_{PF}. Both the general trend and the nice odd–even effect seen on the experimental points are fairly well accounted for by the calculation, even if, here also, the predicted fluctuations are larger than observed. Finally Fig. 9 a) and b) shows the light particle (n, p, α) multiplicity as a function respectively of the PLF′ charge or mass. Low multiplicities are generally predicted, neu-

tron being the most abundant particle accompanying the decaying PLF, with a multiplicity of 2 essentially constant for PLF′ mass and charge lower respectively than 28 a.m.u. and 14 charge unities. On the contrary proton and α multiplicities are generally lower and only for low values of A'_{PF} they reach the unity.

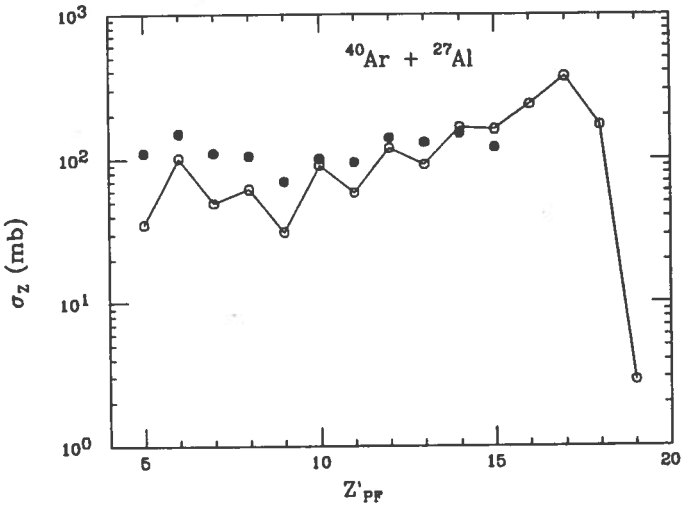

Fig. 8 *Final PLF's production cross section as a function of their charge. Experimental points from ref.* [2].

Care must be taken in comparing these multiplicities with experimental data. Actually, in order to get a meaningfull comparison between experimental and theoretical multiplicities, only particles having a velocity near the one of the coincident PLF and detected in a suitable narrow angle around the direction of the observed PLF should be taken into account. In fact the fast abrasion–ablation model predicts that three different sources of particles are present in the reaction, so that the observed multiplicity can be due to a mixture of them, if not an appropriate selection of particle events is made. At intermediate energies the existing results are a little confused and, as an example, let us mention briefly two recent experiments. In the first of them Bizard et al. [5] have studied the reaction $^{40}Ar + ^{nat}Ag$ at 60 Mev/n, with a particular regard to the charged particle multiplicities accompanying

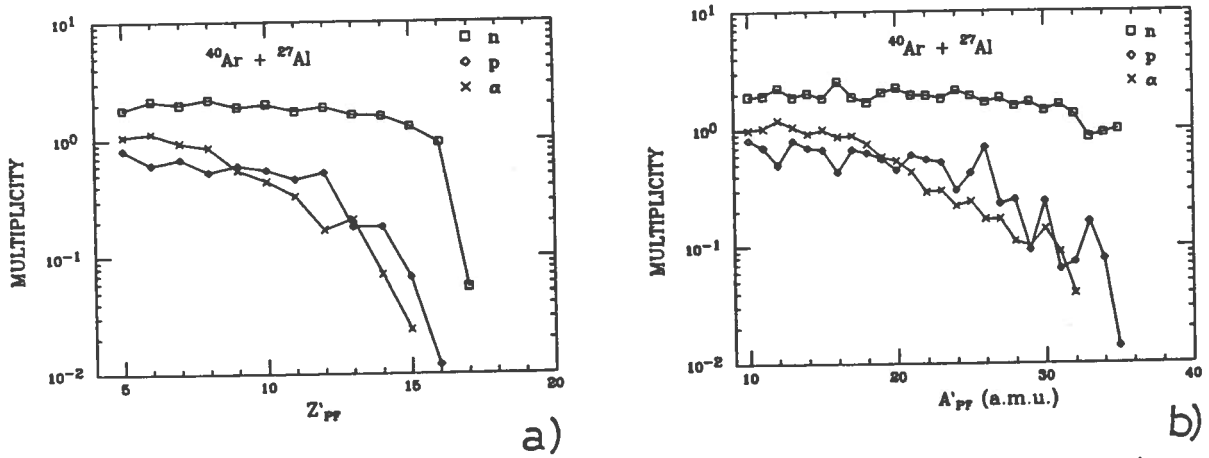

Fig. 9 *Light particle multiplicity as a function of a) PLF′ charge and b) PLF′ mass.*

PLFs detected in forward direction. Charged particles, howewer, were detected in an ample angular range, between $\pm 3°$ and $\pm 30°$. They observed broad light particle charge multiplicities associated with a given fragment charge, and furthermore that for Z'_{PF} near

the value of the projectile ($15 \leq Z'_{PF} \leq 17$), the probability of getting *no (charged) particles* in coincidence with the PLF is very important (between 78% and 47%, following the Z'_{PF} value from 17 to 15). They attributed these probability to a pure transfer reaction, disregarding the fact that neutrons were not measured. We want to recall that, as a result of our calculation, low excited PLFs with mass near the one of the projectile would emit essentially neutrons, so that the above conclusion is, at least in part, false. As an example of the results obtained by our model, in Fig. 10 the light particle multiplicity as a function of the total light particle charge Z_T is reported for two values of the final fragment charge Z'_{PF}, 15 and 10 a.m.u. respectively (the value of $Z_T = 0$ is associated with the emission of only neutrons). As expected, for Z'_{PF} values near the one of the projectile, only

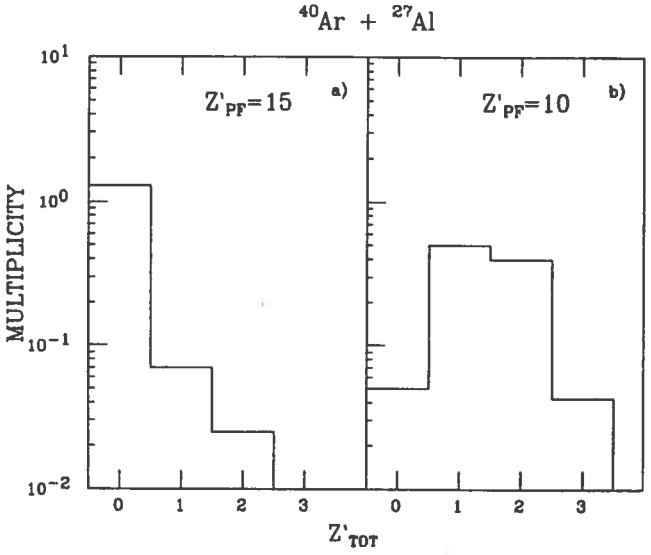

Fig. 10 *Light particle multiplicity as a function of their total charge Z'_T, for final projectile-like fragments of charge respectively 15 and 10.*

neutrons are essentially emitted, while for Z'_{PF} values far from the one of the projectile, neutrons, being still the most abundant particles, are almost always accompanied by light charged particles. In the second experiment, Morjean et al. [6] have studied the reaction $^{40}Ar + Au$ at different intermediate energies, measuring only neutron multiplicities in coincidence with PLF′ detected in the forward direction. In coincidence with a given PLF′ neutron multiplicities as high as 10–15 were measured, while for Z'_{PF} near the charge of the projectile no case of zero neutron multiplicity was found. However, the comparison of the Abrasion–Ablation model with the experimental results is not easy, as in this experiment neutron energy spectra and angular distributions were not mea-

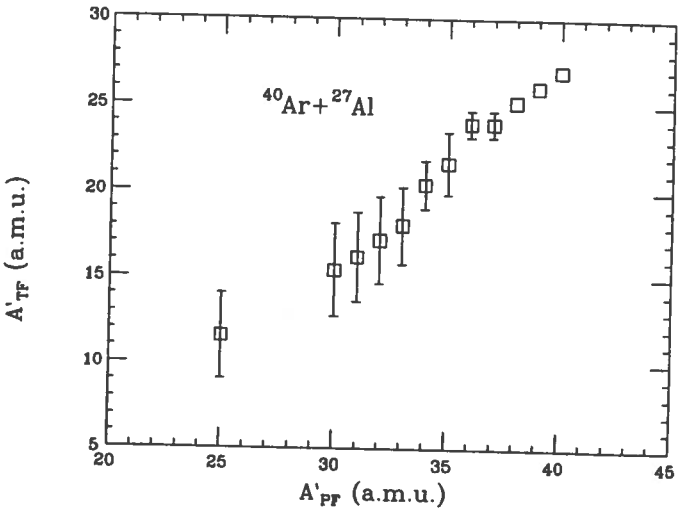

Fig. 11 *Mass–Mass correlation for final projectile and target-like fragments.*

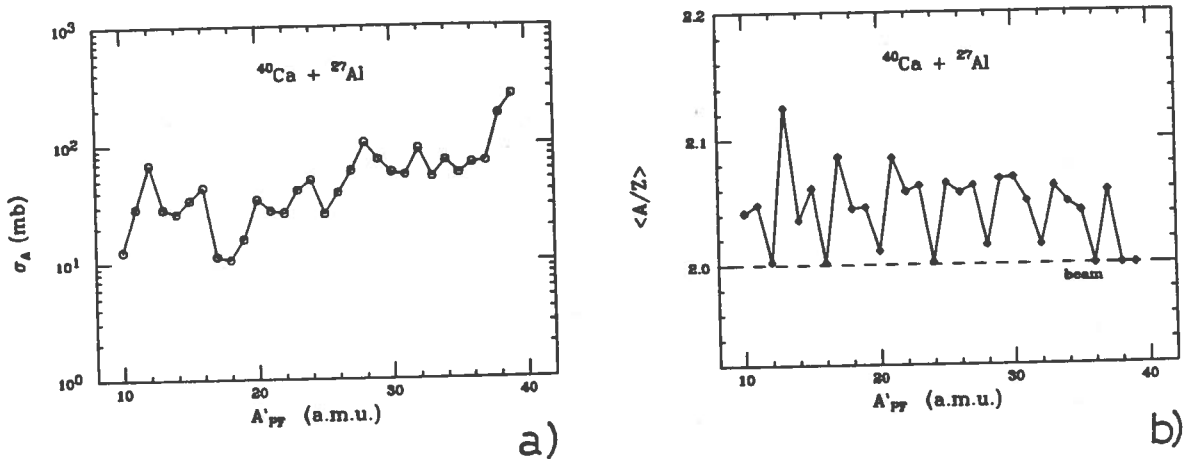

Fig. 12 *a) PLF' production cross section and b) $< A/Z >$ distribution, as a function of the PLF' mass for the reaction $^{40}Ca + ^{27}Al$. The $< A/Z >$ value corresponding to the beam is also shown by a dashed line.*

sured, so that spatial and kinematical correlations between neutrons and PLF are lost. Finally let us consider Fig. 11, in which the mass-mass correlation for PLF and TLF is reported. As shown in ref. [7], the mean trend is fairly reproduced by a fast abrasion model. However, the width associated with each experimental point has not a clear origin, so that it is interesting to ask us if it can be a consequence of the ablation stage. The question is not trivial, and we must have in mind Fig. 3 to see the complexity of the calculations. Consider, as an example, the mass $A'_{PF} = 30$; most of the fragment production cross section is concentrated, for this mass, on the silicon isotope, which is produced, in different extent, by primary PLFs with mass ranging from 31 to 34. On the other side, primary TLFs with mass ranging from $A_{TF} = 18$ to $A_{TF} = 22$ are associated with these primary PLF masses, and furthermore they must be allowed to evaporate particles in order to produce the final observed TLF'. The final result is that TLFs' with mass ranging from 11 to 21 a.m.u. are produced, so that to the initial PLF' mass $A'_{PF} = 30$ we can associate a TLF' mass and width given by $A'_{TF} = 15.4 \pm 3$ a.m.u. This result is considerable, as it constitutes 70% of the observed width. The results are shown in Fig. 11. The accord with the experimental data of ref. [7] is generally good, if we exclude the masses near the projectile and target, where the observed widths are larger than predicted. This last disagreement can be imputed, as already said, on one hand to the presence of transfer-like reactions for very peripheric impact parameters, and on the other hand to a defect of the model which predicts no enough excitation energy for masses near the ones of the projectile and of the target respectively.

b) The $^{40}Ca + ^{27}Al$ reaction

In a process governed by a fast abrasion mechanism, we expect that the projectile's properties, like velocity and N/Z ratio, will influence the features of the final PLF', as observed at relativistic energies [20]. In this respect, as an example, we expect that the PLFs issued from the reaction $^{40}Ca + ^{27}Al$ must manifest different characteristics as compared to the PLFs issued from the reaction $^{40}Ar + ^{27}Al$, due to the different value of

N/Z, 1.0 and 1.22 respectively. To see to which extent these predicted differences between the primary PLFs would persist also after the ablation stage, we have undertaken a series of evaporative calculations for the reaction $^{40}Ca + ^{27}Al$ and compared them to the results obtained for the reaction $^{40}Ar + ^{27}Al$, as above described.

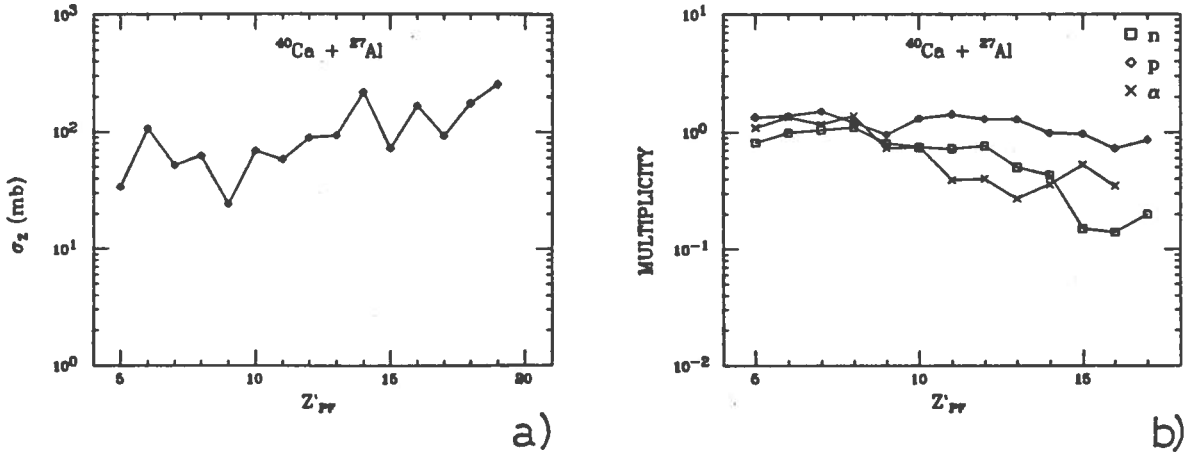

Fig. 13 *a) PLF' production cross section and b) light particle multiplicity as a function of the final PLF' charge for the reaction* $^{40}Ca + ^{27}Al$.

First of all, let's consider Fig. 12a) in which the fragment production is reported as a function of their mass. The global trend is very similar to the one observed for the reaction $^{40}Ar + ^{27}Al$, with a minimum around mass 17–18, after which the cross section is again increasing, with marked maxima at $A'_{PF} = 12$ and 16 a.m.u. Here there are marked pronounced maxima in correspondence of mass numbers 12,16,20,24,28,32, while ^{28}Si and ^{32}S are the most abundant isotopes. In a certain sense the α–structure of the projectile is reflected in the results, as confirmed also in Fig. 12b) in which the ratio $< N/Z >$ is reported as a function of the PLF' mass. The pattern is quite different from the one relative to the reaction $^{40}Ar + ^{27}Al$; pronounced minima are predicted for mass numbers 12,16,20,24,28,32, while almost all the observed $< N/Z >$ values are contained between 2,000 and 2,090 (for the reaction $^{40}Ar + ^{27}Al$, as show in Fig. 5, the same values ranged between 2,000 and 2,150).

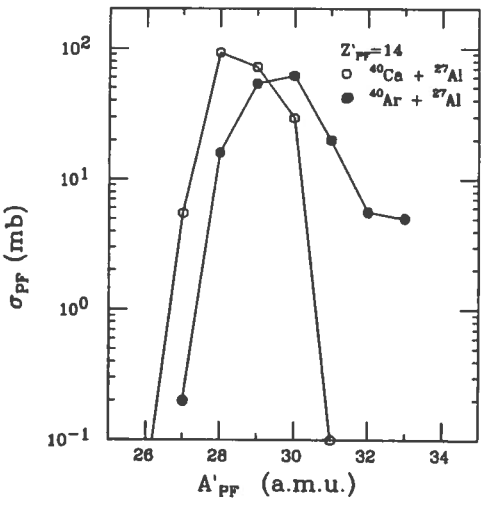

Fig. 14 *Isotopic distribution for a final PLF' of charge 14 relative to the two reactions* $^{40}Ar + ^{27}Al$ *and* $^{40}Ca + ^{27}Al$.

In Fig. 13a) the fragment production cross section is reported as a function of their charge Z'_{PF}. Here also the trend is similar to the one of the reaction $^{40}Ar + ^{27}Al$; to notice

however the abnormal predicted production of the Silicon element ($Z'_{PF} = 14$), compared to the adjacent $Z'_{PF} = 15$ (a factor $\simeq 3$) or $Z'_{PF} = 13$ (a factor $\simeq 2.2$). The odd-even effect is still present. As a consequence of all these results, the isotopic distribution, for each Z'_{PF}, is enriched of isotopes with N/Z ≈ 1. This is clearly seen in Fig. 14 where the isotopic distribution for $Z'_{PF} = 14$ is reported for the two reactions. In general, compared to the isotopic distribution for the reaction $^{40}Ar + ^{27}Al$, it is shifted by $\simeq 1$ a.m.u. toward isotopes less rich in neutron.

Finally Fig. 13b) shows the light particles multiplicity associated to each element Z'_{PF}. Again low multiplicities are associated with final fragments, but now protons are the most abundant particles. Odd–even effect are visible in the proton and alpha multiplicities, but they are opposite in phase. We notice that the odd–even effect observed for the proton multiplicity in the reaction $^{40}Ca + ^{27}Al$ is similar, but opposite in phase, to the one observed for the neutron multiplicity of the reaction $^{40}Ar + ^{27}Al$.

4. Discussion and conclusion

In order to evaluate the effects of the ablation stage on the projectile–like fragments produced by a fast abrasion mechanism, we have carried out a series of evaporative calculations on the primary PLF and TLF issued from the reaction $^{40}Ar + ^{27}Al$. The most important ingredients of the calculations, like excitation energy, charge and production cross section for the primary decaying fragments, have been calculated in the frame of a fast abrasion model. In particular, in order to associate a charge probability to a primary fragment mass, we have developped a very simple method, assuming that each produced fragment mass has a gaussian N/Z distribution, centered on the N/Z ratio of the projectile and whose width we calculate exploiting the charge integrity.

The obtained results are in a fair agreement with existing data at intermediate energy. In particular, with regard to the PLF production as a function of their mass, the general trend is reproduced, with a minimum around mass 18 a.m.u. and an increase of the cross section for lighter mass. On the other hand, the results relative to the PLF production as a function of their charge reproduce the odd–even effect observed at these intermediate energies. Furthermore the shape and width of the isotopic distributions are well accounted for by the calculations.

Many of the above features shown up by final projectile–like fragments reflect the nuclear structure of the initial projectile, as can be seen by making extensive abrasion–ablation calculations on the reaction $^{40}Ca + ^{27}Al$ and by comparing them to the ones relative to the reaction $^{40}Ar + ^{27}Al$. A comparative experimental study of these two reactions would be very interesting to elucidate this point.

Finally, abrasion–ablation calculations carried out on the target–like fragments have allowed some remarkable predictions on the mass-mass correlation between PLF′ and TLF′. In fact a given PLF′ mass is predicted to be correlated with a large TLF′ mass distribution, in accord with the experimental observations. Calculations account for $\approx 70\%$ of these experimental widths.

As a comment to the above summarized results, we can say that the fast abrasion–ablation model, despite his simplicity, predicts many of the characteristics observed in the

projectile fragmentation at intermediate energies. However, one of the drawbacks of this model remains the littleness of excitation energy carried away by the primary fragments, especially for PLF masses near to the one of the projectile. This can be seen in the predicted PLF′ production cross section as a function of both the PLF′ mass or charge, where the large fluctuations can be imputed to this lack of sufficient excitation energy possessed by the primary fragments.

Nor, in this context, the observed PLF′ energy spectra or angular distributions can be explained through the simple evaporation of particles by such a low–excited primary fragments. As an example, a crude estimation of the energy spectra widths made by using the formula of ref. [3] together with the present results of the ablation stage, leads to values that are $\approx 60\%$ of the observed ones. All this seems to suggest that, at these intermediate energies, primary PLF are produced which carry a more substantial excitation energy than geometrically predicted by a simple abrasion–ablation model. A way to overcome this drawback is to use a two–body model, in which all the primary fragments are identified in two highly excited projectile and target [7]. Then the difficulty arises of realize the existence of such equilibrated systems in an energy dominion in which preequilibrium processes are axpected to be more and more important. Compared to this process, a pure fast abrasion mechanism leads to an opposite picture of the reaction, in which the two big PLFs come out cold from the interaction zone, while almost all the excitation energy of the system is concentrated in the overlap zone (fire–ball). Each one of these two extreme and opposite mechanisms can do a satisfactory interpretation of the experimental data,in as much as, very probably, each one of them is one aspect of the involved mechanism.

Coming back now to the fast abrasion–ablation model, we think that, in the light of the above considerations, at least two modifications should be made to render the model more realistic. For PLF masses near the one of the projectile, gentle transfer-like processes of a few particles must be allowed. This process would certainly provide the primary fragments of mass near the one of the projectile (target) with much higher excitation energy, with the result of improving the agreement between the prediction of the model and the experimental results.

For lighter PLF masses, the interaction between PLF and overlap zone must be taken into account, as described, as an example in ref. [21] A part of the particles emitted in the *"explosion"* of the overlap zone is captured by the primary escaping PLF. The more the captured particles, the greater the width of both the angular distribution and the energy spectra, which then result correlated, as observed experimentally. This process, alternatively, can simulate a mechanism characterized by an almost equal flux of particles from projectile to target and viceversa, accompanied by the emission of preequilibrium particles having velocity intermediate betwwen the one of the projectile and the one of the target.

In conclusion, the ablation stage subsequent the abrasion mechanism is able to account for many of the observed experimental features of the projectile-like fragments observed at intermediate energies. However, a careful comparison between calculations and experimental data suggests that the primary projectile fragments must carry a more substantial excitation energy than predicted by a purely geometric abrasion model, in order to get a better agreement between theory and experiment.

References

[1] For an exhaustive survey of the projectile fragmentation at intermediate energies see, for instance:
R. Dayras: *Journal de Physique*, **C4–13**, (1986).
D. Guerreau: . *Nucl. Phys. A*, **447**, 37c, (1986).

[2] R. Dayras, A. Pagano, J. Barrette, B. Berthier, D.M. De Castro Rizzo, E. Chavez, O.Cisse, R. Legrain, M.C. Mermaz, E.C. Pollacco, H. Delagrange, W. Mittig, B. Heusch, R. Coniglione, G. Lanzanò and A. Palmeri: *Nucl. Phys. A*, **460**, 299 (1986).

[3] G. Lanzanò, A. Pagano and F. Gadi *Nuovo Cimento* **99** A, 839 (1988).

[4] J. Gomez Del Campo, J. Barrette, R.A. Dayras, J.P.Wieleczko, E. Pollacco, F. Saint-Laurent, M. Toulemonde, N. Neskocic and R. Ostojec: *Bull. Am. Phys. Soc.*, **30**, 1283 (1985)

[5] G. Bizard, R.Brou, H. Doubre, A. Drouet, F. Guilbaut, F. Hanappe, J.M. Harasse, J.L. Laville, C. Lebrun, A. Oubahadou, J.P. Patry, J. Peter, G. Ployart, J.C. Steckmeyer and B. Tamain: *Phys. Lett. B*, **172**, 301, (1986).

[6] M. Morjean, J. Frehaut, D. Guerreau, J.L. Charvet, G. Duchene, H. Doubre, J. Galin, G. Ingold, D. Jacquet, U. Jahnke, D.X. Jiang, B. Lott, C. Magnago, Y. Patin, J. Pouthas, Y. Pranal and J.L. Uzureau: *Phys. Lett. B*, **203**, 215 (1988).

[7] R. Dayras, R. Coniglione, J. Barrette, B. Berthier, D.M. De Castro Rizzo, O.Cisse, F. Gadi, R. Legrain, M.C. Mermaz, H. Delagrange, W. Mittig, B. Heusch, G. Lanzanò and A. Pagano: *Phys. Rev. Lett.* , **62**, 1017, (1989).

[8] J. Gosset, H.H. Gutbrod, W.G. Meyer, A.M. Poskanzer, A. Sandoval, R. Stock and G.D. Westfall: *Phys. Rev. C*, **16**, 629 (1977).

[9] J.D. Bowman, W.J. Swiatecki and C.F. Tsang, *LBL Report* No LBL-2908, (1973) (unpublished).

[10] A. Bonasera, M. Di Toro and C. Grègoire: *Nucl. Phys. A*, **463**, 653 (1987).

[11] L.F. Oliveira, R. Donangelo, J.O. Rasmussen: *Phys. Rev. C*, **19**, 826, (1979).

[12] D.J. Morrissey, W.R. Marsh, R.J. Otto, W. Loveland and G.T. Seaborg: *Phys. Rev. C*, **18**, 1267 (1978).

[13] E.J. Moniz, I. Sick et al.: *Phys. Rev. Lett.*, **26**, 445 (1971).

[14] D. Guerreau, V. Borrel, D. Jacquet, J. Galin, B. Gatty and X. Tarrago: *Phys. Lett.*, **131B**, 293 (1983).

[15] F. Puhlhofer: Program CASCADE.

[16] R. Dayras: Program ABRADE.

[17] M.C. Mermaz, R. Dayras, J. Barrette, B. Berthier, D.M. De Castro Rizzo, O.Cisse, R. Legrain, A. Pagano, E.C. Pollacco, H. Delagrange, W. Mittig, B. Heusch, G. Lanzanò and A. Palmeri: *Nucl. Phys. A*, **441**, 129 (1985).

[18] V. Borrel, D. Guerreau, J. Galin, B. Gatty, D. Jacquet and X. Tarrago: *Z. Phys. A*, **314**, 191 (1983).

[19] F. Rami: These d' Etat, Université de Strasburg (1985) unpublished.

[20] G.D. Westfall et al. :*Phys. Rev. Lett.*, **43**, 1859 (1979).

[21] J.P. Bondorf, J. De, G. Fai and A.O.T. Karvinen: *Nucl. Phys. A*, **430**, 445 (1984).